Observational study

Clin Ter 2024; 175 (1):20-25 doi: 10.7417/CT.2024.5029

The effectiveness of diffusion kurtosis imaging metrics for distinguishing between brainstem glioma and cerebellar medulloblastoma

N. Minh Duc[1]

[1]Department of Radiology, Pham Ngoc Thach University of Medicine, Ho Chi Minh City, Vietnam

Abstract

Background. In some clinical situations, distinguishing between cerebellar medulloblastoma and brainstem glioma is important. We assessed whether diffusion kurtosis imaging (DKI) metrics could be used to distinguish cerebellar medulloblastomas from brainstem gliomas in children.

Patients and methods. This prospective study was approved by the institutional review board. Seventy patients were separated into two groups according to eventual diagnosis: brainstem glioma (n = 30) and cerebellar medulloblastoma (n = 40). Both groups underwent brain magnetic resonance imaging (MRI), including DKI. The Kurtosis value for the tumor region and the ratio between Kurtosis values between the tumor and the normal parenchyma (rKurtosis) were compared between groups using the Mann–Whitney U test. Receiver operating characteristic curve analysis and the Youden's Index were applied to identify a cutoff value for distinguishing between the two tumor types, and the area under the curve (AUC), sensitivity, and specificity for the selected cutoff value were calculated.

Results. Compared with brainstem gliomas, cerebellar medulloblastomas had significantly higher Kurtosis and rKurtosis values ($p < 0.05$). Medulloblastoma could be differentiated from brainstem gliomas using a Kurtosis value of 0.91 or an rKurtosis value of 0.90, both of which achieved 100% sensitivity, 96.7% specificity, and AUC values of 0.990

Conclusions. DKI measurements can contribute to distinguishing between cerebellar medulloblastoma and brainstem glioma in children.
Clin Ter 2024; 175 (1):20-25 doi: 10.7417/CT.2024.5029

Keywords: *Cerebellar medulloblastoma, brainstem glioma, magnetic resonance imaging, diffusion kurtosis imaging*

Introduction

Brain tumors are the second-most common malignancy in children, behind acute leukemia. Brain tumors can be either supratentorial or infratentorial in nature, but infratentorial tumors are more common, occurring in approximately 60% of all juvenile brain tumors. Glioma tumors commonly present in the brainstem region, whereas medulloblastoma more commonly occurs in the cerebellum[1,2].

Medulloblastomas can also originate in or invade the brainstem, resulting in the misdiagnosis of medulloblastoma as brainstem glioma in early literature[1,3,4]. In patients with medulloblastoma treated with radiotherapy, determining whether brainstem lesions represent disease relapse or are new brainstem gliomas can be challenging[5,6]. Different prognoses and treatment plans are needed for these illnesses. However, distinguishing between these two types of neoplasms is essential for ensuring the accurate planning of therapeutic approaches for enhanced treatment outcomes[1-6].

The classification of different types of brain tumors often relies on histopathological analysis. However, obtaining surgical biopsies from brain regions is associated with high risks of morbidity and death. Inadequate intraoperative microscopic diagnosis occurs in approximately 8% of brain neoplasm cases. Accurate neuroimaging able to distinguish tumor types can contribute to improved diagnosis prior to the start of therapy[7]. Magnetic resonance imaging (MRI) is regarded as the safest imaging modality for the identification of juvenile brain tumors due to its non-invasive nature and because MRI does not expose the child to ionizing radiation. Diffusion-weighted imaging (DWI) and diffusion tensor imaging (DTI) are well-established techniques that are often applied to the radiological evaluation of brain tumors. However, the staging utility of these diffusion-based sequences remains suboptimal[8]. DWI and DTI both assume that water molecule diffusion is the result of random Brownian motion. Based on this assumption, the probability distribution function (PDF) suggests that a proton's likelihood of diffusing between two places during a given time period follows a Gaussian distribution. The apparent diffusion coefficient in DTI is derived using a direction-dependent method based on the standard deviation of the PDF[9,10]. Although the Gaussian model used for DWI and DTI is accurate for pure liquids, these techniques ignore the impacts of environmental factors *in vivo*. The complex cytoarchitecture of organic tissues consists of numerous compartments, cell types, and intracellular components, which can affect the movements of both water and lipids, which is not considered by the Gaussian

Correspondence: Nguyen Minh Duc, Department of Radiology, Pham Ngoc Thach University of Medicine, Ho Chi Minh City, Vietnam
Email: bsnguyenminhduc@pnt.edu.vn. https://orcid.org/0000-0001-5411-1492

Copyright © Società Editrice Universo (SEU)
ISSN 1972-6007

model used for DWI and DTI. Therefore, the actual PDF displays non-Gaussian behavior, and the difference between the actual PDF and the estimated Gaussian PDF can be calculated using the dimensionless statistical metric known as Kurtosis. The degree of directed, non-Gaussian diffusion can be determined using diffusion kurtosis imaging (DKI), a unique extension of diffusion tensor imaging (DTI)[11,12]. Microstructural differences between different grades of gliomas are expected to result in different Kurtosis values, indicating that the Kurtosis value may represent a more accurate, non-invasive biomarker for glioma staging, although the actual physiological basis of DKI remains unknown[9,13]. This study was conducted whether DKI metrics could be applied to distinguishing between cerebellar medulloblastoma and brainstem glioma.

Methods

Patient identification

The Institutional Review Board of Children's Hospital 02 approved this prospective study (Ref: 352/NĐ2-CĐT). Written informed consent was received from authorized guardians of all patients prior to performing the MRI scans. This study was performed at Children's Hospital 02 from February 2019 to February 2021. Seventy patients were enrolled in this study, divided into two groups according to eventual diagnosis, including 30 patients diagnosed with brainstem glioma and 40 patients diagnosed with cerebellar medulloblastoma. Brainstem glioma was diagnosed based on consensus among neuroradiologists and neurosurgeons. Cerebellar medulloblastoma was diagnosed according to the histopathological outcomes of surgical specimens or biopsies.

Anesthesia process

All patients in this study were required to fast for at least 6 hours prior to initiating the anesthesia process. The patient was placed in a supine position on the MRI table. The physician administered midazolam (Hameln Pharm GmbH, Germany; 5 mg/ml) intravenously, at a dose of 0.1 mg/kg and 1% propofol (Fresofol, Fresenius Kabi GmbH, Austria; 10 mg/ml), at a dose of 3 mg/kg.

MRI procedure

In this study, all patients were scanned with a 1.5 Tesla MRI machine (Multiva, Philips, Best, The Netherland) and assessed using the DWI sequence, with the following parameters: repetition time (TR): shortest; echo time (TE): shortest; flip angle: 90 degrees; slice thickness: 5 mm; gap: 1 mm; field of view: 230 mm × 230 mm; matrix: 144 mm × 90 mm; plane: axial; number of Acquisitions: 2; b values: 0, 25, 50, 100, 200, 1000, and 1500; duration: 3.43 minutes.

Clinical data

The Advanced Diffusion Analysis mode, available in the Philips Intellispace Portal, version 11, was used to analyze defined regions of interest (ROIs) in tumor tissues and the adjacent, normal-appearing parenchyma for the calculation of Kurtosis values (Figs. 1 and 2). This study used a single-

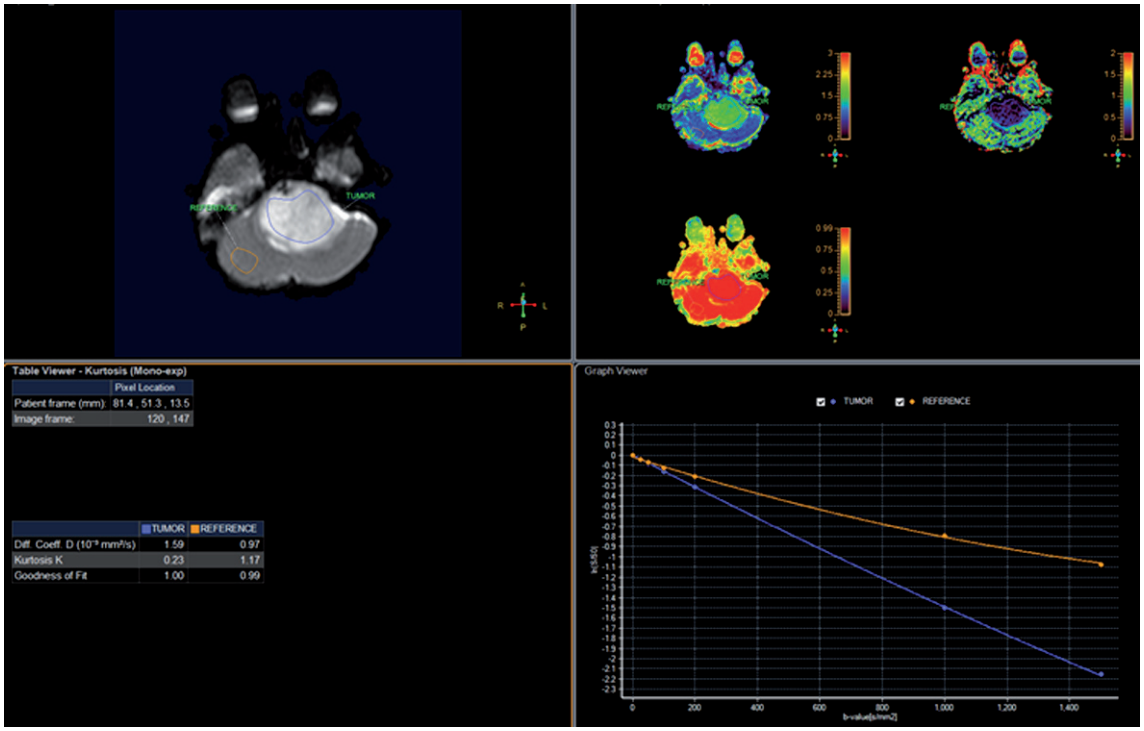

Fig. 1. A 6-year-old male patient with a tumor located in the pons, which was diagnosed as a brainstem glioma. DKI was analyzed by drawing ROIs within the tumor region (blue ROI) and within the normal parenchyma (orange ROI). The Kurtosis values for the tumor and the parenchyma were 0.23 and 1.17, respectively.

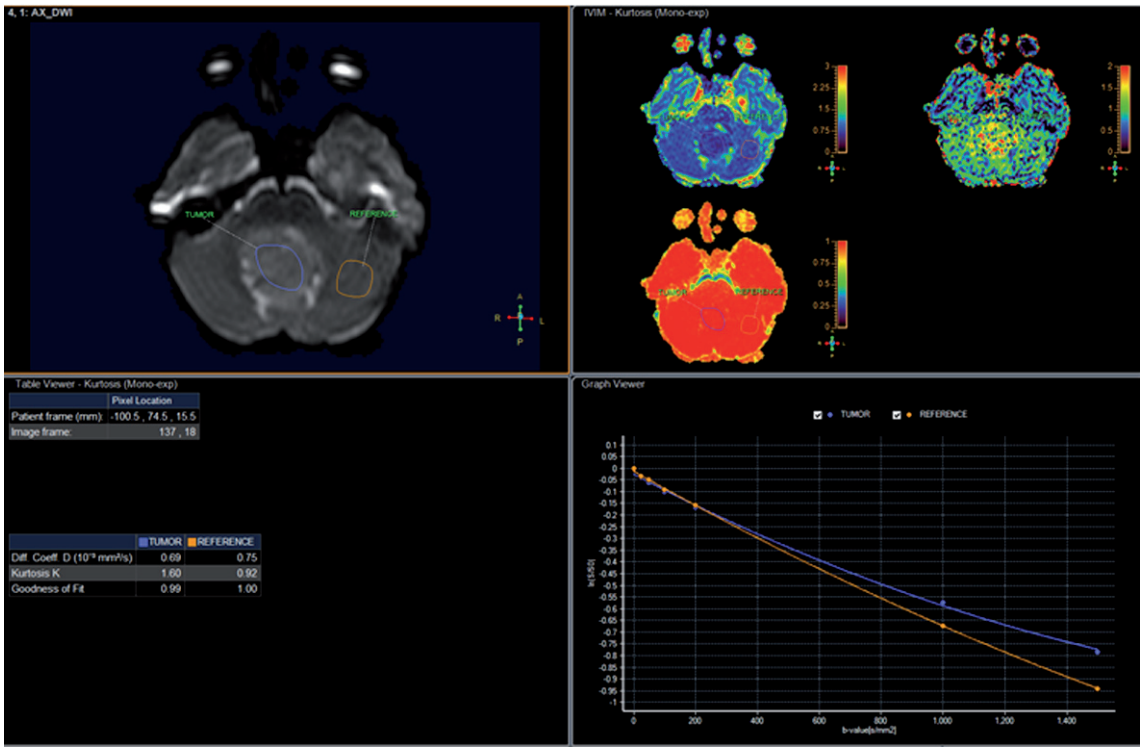

Fig. 2. An 8-year-old male patient with a tumor inside the fourth ventricle, which was confirmed to be medulloblastoma following surgery. DKI was analyzed by drawing ROIs within the tumor region (blue ROI) and within the normal parenchyma (orange ROI). The Kurtosis values for the tumor and the parenchyma were 1.60 and 0.92, respectively.

ROI analysis performed in an unblinded manner. The ratio between the Kurtosis values of the tumor and the adjacent parenchyma was calculated by dividing the signal intensity obtained from the tumor ROI by the signal intensity obtained from an ROI placed in the adjacent, normal-appearing parenchyma. The tumor to parenchyma Kurtosis value is referred to as the rKurtosis value.

Statistical analysis

SPSS software version 26 (IBM Corp, Armonk, New York, USA) was used for statistical analysis. Quantitative variables are presented as the median and interquartile range. We compared quantitative variables using the Mann–Whitney U test. Receiver operating characteristic (ROC) curve analysis and Youden's Index were used to evaluate the cutoff point for distinguishing between tumor types and to calculate the area under the curve (AUC), sensitivity, and specificity when the selected cutoff point was applied. Differences were considered significant for *p*-values < 0.05.

Results

A total of 70 patients were divided into two groups, including 30 (42.86%) patients with brainstem glioma and 40 (57.14%) patients with cerebellar medulloblastoma. The median ages were 6 years for the brainstem glioma group and 7 years for the cerebellar medulloblastoma group. The male:female ratios were 16: 14 for the brainstem glioma group and 25: 15 for the cerebellar medulloblastoma group.

As shown in Table 1, the Kurtosis and rKurtosis values for cerebellar medulloblastoma were significantly higher than those for brainstem glioma ($p < 0.05$).

A cutoff Kurtosis value of ≥0.91 and a cutoff rKurtosis value of ≥0.90 was employed to distinguish medulloblastomas from brainstem gliomas, which resulted in 100% sensitivity, 96.7% specificity, and an AUC of 0.990 for both parameters (Figs. 3 and 4, Table 2).

Discussion

To date, no other studies have employed DKI for the differentiation of cerebellar medulloblastoma from brainstem glioma. Our study found that brainstem glioma and cerebellar medulloblastoma had median Kurtosis values of 0.49 and 1.41 ($p < 0.05$), respectively, and median rKurtosis values of 0.48 and 1.30 ($p < 0.05$), respectively. Cutoff Kurtosis and rKurtosis values of ≥0.91 and ≥0.90, respectively, were able to distinguish between brainstem glioma and cerebellar medulloblastoma with sensitivities of 100%, specificities of 96.7%, and AUC values of 0.990. In two previous meta-analyses examining the diagnostic value of DKI, the Kurtosis value was estimated to have pooled AUC values of 0.94 and 0.96 for glioma grading[14,15].

A meta-analysis conducted by Abdalla et al,[16] which

Table 1. Comparison of basic characteristics between cerebellar medulloblastoma and brainstem glioma

Parameters	Brainstem glioma (n = 30)	Cerebellar medulloblastoma (n = 40)	p-value
Kurtosis	0.49 (0.29)	1.41 (0.30)	< 0.001
rKurtosis	0.48 (0.31)	1.30 (0.48)	< 0.001

Values displayed represent the mean (interquartile range)

Table 2. ROC analysis of DTI metrics for the diagnosis of cerebellar medulloblastomas

Parameters	Cutoff point	AUC	Sensitivity	Specificity	95% CI
Kurtosis	≥0.91	0.990	100	96.7	0.970–1.000
rKurtosis	≥0.90	0.990	100	96.7	0.970–1.000

ROC, receiver operating characteristic; DTI, diffusion tensor imaging; AUC; area under the curve; CI, confidence interval

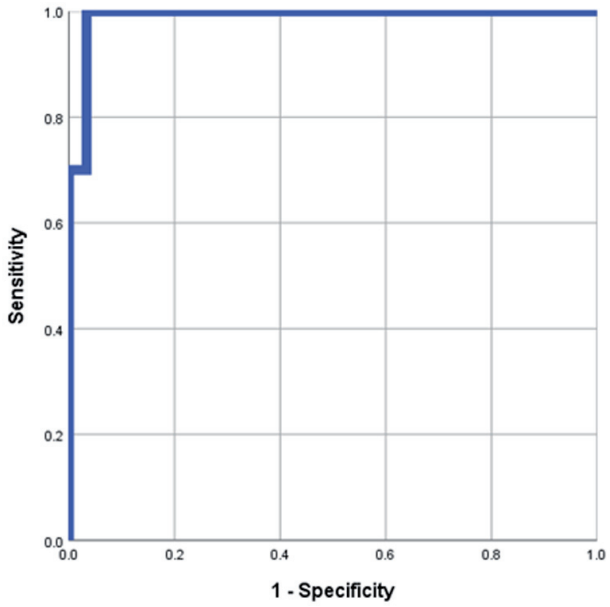

Fig. 3. The receiver operating characteristic curve for the Kurtosis value.

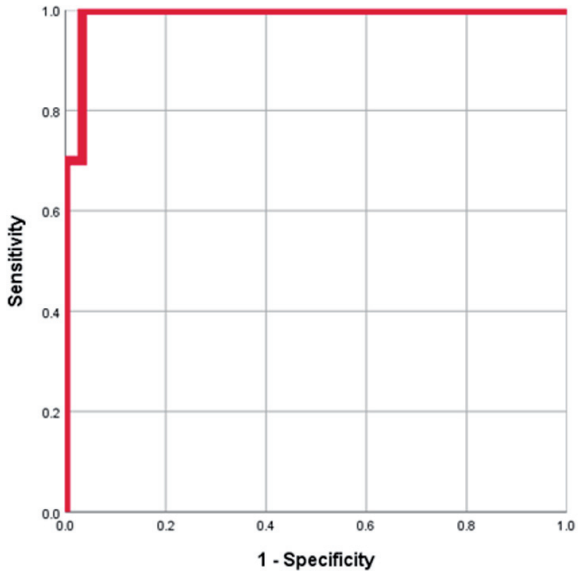

Fig. 4. The receiver operating characteristic curve for the relative Kurtosis value

included 19 studies, found a significant mean difference of 0.22 (95% confidence interval [CI]: 0.19–0.25) between the Kurtosis values of high-grade and low-grade gliomas based on a mean difference analysis of the results from 12 studies[16]. These findings are similar to those reported by Falk Delgado et al[14], who analyzed 10 studies and reported a significant difference 0.17 (95% CI: 0.11–0.22) in Kurtosis values of high-grade and low-grade gliomas. In 4 of the 19 studies included in a systematic review, the ability of DKI to stratify patients according to isocitrate dehydrogenase (*IDH*) mutation status based on the 2016 WHO classification guidelines[13,17-19]. These investigations found a significant difference in Kurtosis values between patients with wild-type and mutant *IDH*, indicating that DKI could be used as a marker for IDH phenotyping.

Despite being associated with various histological types, according to the 2016 WHO classification guidelines, all medulloblastomas are classed as grade-IV tumors, which are considered the most dangerous and have the poorest prognosis in both children and adults. By contrast, brainstem gliomas can be graded between II and IV, and the classification parameters can sometimes be debated. In addition,

children diagnosed with brainstem glioma tend to have a better prognosis than adults[20-22]. The Kurtosis value obtained using DKI, an extension of DTI, is thought to be influenced by differences in the tissue microstructure and is considered proportionate to the heterogeneity and complexity of the tissue microstructure[23-25]. DKI has demonstrated effectiveness in diagnosing infarction, traumatic brain injury, neoplasms, neurodegenerative illness, and demyelinating disorders[24]. Therefore, DKI may represent a more informative imaging modality than either DWI or DTI for identifying potential microstructural changes in tissues and cells.

Extremely cancerous brain tumors, such as medulloblastomas, are characterized by rapid cell division and high density[23-27]. Reductions in signal output are associated with increasing limitations placed on the free passage of water molecules through inter- and intracellular gaps. Therefore, although the Kurtosis and rKurtosis values tend to be larger for medulloblastoma, the diffusion velocity is reduced in these tumors. By contrast, brainstem gliomas are less dense[23-27], with fewer restrictions on hydrogen proton transport in the intercellular regions. As a result, the Kurtosis and rKurtosis values are lower in brainstem gliomas than in medulloblastomas, but the diffusion rates associated with brainstem gliomas are higher[23-27].

The small sample size and the recruitment of patients from a single center are two limitations of our study. In addition, this study did not perform DKI histogram tumor analysis or examine tumor morphological characteristics. Additionally, all patients with brainstem glioma were diagnosed clinically[28,29], without the performance of any histological study, in accordance with our hospital's treatment guidelines. We recommend additional studies with larger samples and multicenter involvement to verify our current findings.

Conclusion

In conclusion, DKI was very useful in distinguishing between cerebellar medulloblastoma and brainstem glioma. With AUC values of 0.990, both the Kurtosis and rKurtosis values were very effective in differentiating cerebellar medulloblastoma from brainstem glioma. To confirm our current findings, additional research with larger sample sizes and multicenter participation should be conducted.

Acknowledgment

We would like to express our gratitude to Dr. Dang Do Thanh Can, Mrs. Dang Thi Bich Ngoc for their assistance and technical support in completing this research.

Ethical approval and declaration of patient consent

Institutional review board of Children's Hospital 2 approved this prospective study (Ref: 352/NĐ2-CĐT). Written informed consent was obtained from the legal guardian of all participating patients.

Data availability statement

Data sharing is not applicable to this article as no datasets were generated or analysed during the current study.

Conflict of interests

There are no conflicts of interest to declare.

Financial support and sponsorship

Nil.

Author contributions

Nguyen Minh Duc performed all essential steps to complete this manuscript.

References

1. Jallo GI, Biser-Rohrbaugh A, Freed D. Brainstem gliomas. Childs Nerv Syst 2004; 20:143-153
2. Ostrom QT, de Blank PM, Kruchko C, et al. Alex's Lemonade Stand Foundation Infant and Childhood Primary Brain and Central Nervous System Tumors Diagnosed in the United States in 2007-2011. Neuro Oncol 2015; 16(Suppl 10): x1-x36
3. Ahn MS, Jackler RK. Exophytic brain tumors mimicking primary lesions of the cerebellopontine angle. Laryngoscope 1997; 107:466-471
4. Yoshimura J, Nishiyama K, Fukuda M, et al. Adult cerebellopontine angle medulloblastoma originating in the pons mimicking focal brainstem tumor. J Neuroimaging 2009; 19(4):385-387
5. Yamanaka R, Hayano A, Kanayama T. Radiation-induced gliomas: a comprehensive review and meta-analysis. Neurosurg Rev 2018; 41:719-731
6. Gits HC, Anderson M, Stallard S, et al. Medulloblastoma therapy generates risk of a poorly-prognostic H3 wild-type subgroup of diffuse intrinsic pontine glioma: a report from the International DIPG Registry. Acta Neuropathol Commun 2018; 6:67
7. Winkler D, Lindner D, Richter A, et al.The value of intraoperative smear examination of stereotaxic brain specimens. Minim Invasive Neurosurg 2006; 49:353-356
8. Usinskiene J, Ulyte A, Bjørnerud A, et al. Optimal differentiation of high- and low-grade glioma and metastasis: a meta-analysis of perfusion, diffusion, and spectroscopy metrics. Neuroradiology 2016; 58:339-350
9. Van Cauter S, Veraart J, Sijbers J, et al. Gliomas: diffusion kurtosis MR imaging in grading. Radiology 2012; 263: 492-501
10. Basser PJ, Mattiello J, LeBihan D. MR diffusion tensor spectroscopy and imaging. Biophys J 1994; 66:259-267
11. Jensen JH, Helpern JA, Ramani A, et al. Diffusional kurtosis imaging: the quantification of non-gaussian water diffusion by means of magnetic resonance imaging. Magn Reson Med 2005; 53:1432-1440
12. Lu H, Jensen JH, Ramani A, et al. Three-dimensional characterization of non-gaussian water diffusion in humans using diffusion kurtosis imaging. NMR Biomed 2006; 19: 236-247
13. Hempel JM, Bisdas S, Schittenhelm J, et al. In vivo molecular profiling of human glioma using diffusion kurtosis imaging. J Neurooncol 2017; 131:93-101
14. Falk Delgado A, Nilsson M, van Westen D, et al. Glioma Grade Discrimination with MR Diffusion Kurtosis Imaging: A Meta-Analysis of Diagnostic Accuracy. Radiology 2018; 287:119-127

15. Huang R, Chen Y, Li W, Zhang X. An evidence-based approach to assess the accuracy of diffusion kurtosis imaging in characterization of gliomas. Medicine (Baltimore) 2018; 97:e13068
16. Abdalla G, Dixon L, Sanverdi E, et al. The diagnostic role of diffusional kurtosis imaging in glioma grading and differentiation of gliomas from other intra-axial brain tumours: a systematic review with critical appraisal and meta-analysis. Neuroradiology 2020; 62:791-802
17. Hempel JM, Schittenhelm J, Bisdas S, et al. In vivo assessment of tumor heterogeneity in WHO 2016 glioma grades using diffusion kurtosis imaging: Diagnostic performance and improvement of feasibility in routine clinical practice. J Neuroradiol 2018; 45:32-40
18. Hempel JM, Schittenhelm J, Brendle C, et al. Histogram analysis of diffusion kurtosis imaging estimates for in vivo assessment of 2016 WHO glioma grades: A cross-sectional observational study. Eur J Radiol 2017; 95:202-211
19. Hempel JM, Schittenhelm J, Brendle C, et al. Effect of Perfusion on Diffusion Kurtosis Imaging Estimates for In Vivo Assessment of Integrated 2016 WHO Glioma Grades: A Cross-Sectional Observational Study. Clin Neuroradiol 2018; 28:481-491
20. Louis DN, Perry A, Reifenberger G, et al. The 2016 World Health Organization Classification of Tumors of the Central Nervous System: a summary. Acta Neuropathol 2016; 131: 803-820
21. Kaatsch P, Rickert CH, Kuhl J, et al. Population-based epidemiologic data on brain tumors in German children. Cancer 2001; 92:3155–3164
22. Sanders RP, Kocak M, Burger PC, et al. High-grade astrocytoma in very young children. Pediatr Blood Cancer 2007; 49:888–893
23. Zhuo J, Xu S, Proctor JL, et al. Diffusion kurtosis as an in vivo imaging marker for reactive astrogliosis in traumatic brain injury. Neuroimage 2012; 59:467-477
24. Steven AJ, Zhuo J, Melhem ER. Diffusion kurtosis imaging: an emerging technique for evaluating the microstructural environment of the brain. AJR Am J Roentgenol 2014; 202: W26-33
25. Tietze A, Hansen MB, Østergaard L, et al. Mean Diffusional Kurtosis in Patients with Glioma: Initial Results with a Fast Imaging Method in a Clinical Setting. AJNR Am J Neuroradiol 2015; 36:1472-1478
26. Minh Thong P, Minh Duc N. The Role of Apparent Diffusion Coefficient in the Differentiation between Cerebellar Medulloblastoma and Brainstem Glioma. Neurol Int 2020; 12:34-40
27. Duc NM. The role of diffusion tensor imaging metrics in the discrimination between cerebellar medulloblastoma and brainstem glioma. Pediatr Blood Cancer 2020; 67:e28468